

Gene expression changes in the brain of a Cushing's syndrome mouse model

Jorge Miguel Amaya¹  | Eva M. G. Viho¹  | Hetty C. M. Sips¹ | Reshma A. Lalai¹ | Isabelle Sahut-Barnola² | Typhanie Dumontet²  | Nathanaëlle Montanier²  | Alberto M. Pereira¹  | Antoine Martinez²  | Onno C. Meijer¹ 

¹Department of Internal Medicine, Division of Endocrinology, Leiden University Medical Center, Leiden, The Netherlands

²Génétique Reproduction et Développement, Université Clermont-Auvergne, CNRS, INSERM, Clermont-Ferrand, France

Correspondence

Onno C. Meijer, Department of Medicine, Leiden University Medical Center, Albinusdreef 2, 2333 ZA Leiden, The Netherlands.
Email: o.c.meijer@lumc.nl

Funding information

Agence Nationale pour la Recherche, Grant/Award Numbers: ANR-14-CE12-0007-01, ANR-18-CE14-0012-02; Consejo Nacional de Ciencia y Tecnología, Grant/Award Number: 440584

Abstract

Excess glucocorticoid exposure affects emotional and cognitive brain functions. The extreme form, Cushing's syndrome, is adequately modelled in the AdKO_{2.0} mouse, consequential to adrenocortical hypertrophy and hypercorticosteronemia. We previously reported that the AdKO_{2.0} mouse brain undergoes volumetric changes that resemble closely those of Cushing's syndrome human patients, as well as changes in expression of glial related marker proteins. In the present work, the expression of genes related to glial and neuronal cell populations and functions was assessed in regions of the anterior brain, hippocampus, amygdala and hypothalamus. Glucocorticoid target genes were consistently regulated, including CRH mRNA suppression in the hypothalamus and induction in amygdala and hippocampus, even if glucocorticoid receptor protein was downregulated. Expression of glial genes was also affected in the AdKO_{2.0} mouse brain, indicating a different activation status in glial cells. Generic markers for neuronal cell populations, and cellular integrity were only slightly affected. Our findings highlight the vulnerability of glial cell populations to chronic high levels of circulating glucocorticoids.

KEYWORDS

brain, Cushing's syndrome, glia, glucocorticoid, neuron

1 | INTRODUCTION

Glucocorticoid stress hormones are potent regulators of brain function. Their effects are mediated via two receptor types, high affinity mineralocorticoid receptors (MRs) and lower affinity glucocorticoid receptors (GRs).¹ Particularly, GRs are expressed in many different brain regions and cell types.^{2,3} Glucocorticoid effects in hippocampus, amygdala and prefrontal cortex^{4,5} are subject to extensive research in relation to cognitive and emotional functioning.⁶ In the hypothalamus, glucocorticoids are pivotal for the

negative feedback regulation of the hypothalamus pituitary adrenal axis. While transient glucocorticoid effects in the context of circadian rhythmicity and acute stress responses are adaptive, loss of circadian rhythmicity and chronic increased exposure put the brain at risk for disease.⁷

In humans, chronic overexposure to glucocorticoids leads to Cushing's syndrome (CS). As such, CS patients may be considered a model for the potential effects of chronic exposure to both stress-induced endogenous glucocorticoids and—as far as GR activation goes—synthetic glucocorticoids. CS patients may present with both

This is an open access article under the terms of the Creative Commons Attribution-NonCommercial-NoDerivs License, which permits use and distribution in any medium, provided the original work is properly cited, the use is non-commercial and no modifications or adaptations are made.

© 2022 The Authors. *Journal of Neuroendocrinology* published by John Wiley & Sons Ltd on behalf of British Society for Neuroendocrinology.

psychiatric complications^{8–10} and cognitive impairments,^{11–13} and they have extensive volumetric changes in the brain.^{14–16} Some of these changes persist even in a remitted stage.^{17–19}

Experimentally, we have developed a mouse model that not only replicates peripheral signs of CS,^{20–22} but also displays brain volumetric changes mirroring what has been observed in the human studies. In these mice, which develop bilateral adrenocortical hyperplasia as a consequence of protein kinase A (PKA) overactivity, we were also able to show substantial changes in microglia, astrocytes and oligodendrocyte protein markers in both grey and white matter structures, namely cortex, hippocampus, and corpus callosum.²³ We considered that assessment of changes in gene expression could provide with information to extend our previous findings, and unveil their potential mechanisms. An expanded description of changes in the brain caused by chronic exposure to glucocorticoids, would help to define specific vulnerabilities of the different cell types, and in consequence would allow to weigh potential therapeutic targets. With the present study we tested the hypothesis that the changes we observed previously could be related to cell-specific transcriptional differences of cellular “state,” rather than constitutively expressed “trait” markers in diverse brain areas, including hippocampus, amygdala and hypothalamus. To this end, we defined groups of genes belonging to specific cell types based on single cell sequencing data from the Allen Brain Atlas (Figure 2). We also assessed the expression of genes known to be regulated by GR activation, and genes related to oxidative stress pathways. Additionally, we explored possible alterations in neuronal populations in areas that showed changes in the marker gene NeuN.

2 | MATERIALS AND METHODS

2.1 | Mice

Litters from wild-type and AdKO_{2.0} mice were bred and raised as previously described.²³ From each genotype, mice from both sexes were sacrificed at 8–10 weeks of age. Mice bred in-house and maintained on a mixed sv129-C57Bl/6 genetic background were housed in a 12:12 light–dark cycle (ZTO at 07:00 h), in 1145 T NEXT for Mice cages (Techniplast), Mice were fed normal, commercial rodent chow and provided with water ad libitum. Cages were supplied with a minidome, and Lab Aspen maxi bedding (Serlab) was changed every 2 weeks. After weaning, mice were kept in siblings with a minimum of three and a maximum of four animals per cage. Prior to tissue collection, mice were humanely euthanized by decapitation and all efforts were made to minimize suffering. Sacrifices were performed between 08:00 and 09:00 h. Brains were extracted from skulls and placed in dry ice for instant freezing. Afterwards, they were stored at -80°C until further processing. Blood from the trunk was collected after less than 30 s of handling to minimize stress. Basal plasma corticosterone levels were determined using commercially available ELISA kit (AR E-8100) (LDN). AdKO_{2.0} refers to *Sf1-Cre::Prkar1a^{fl/fl}* as previously described, and WT refers to littermate control animals.^{21–23} All animal work was conducted according to French and European directives for use and care of animals for research purposes and received the approval from

the French ministry of higher education, research and innovation (APAFIS#21153–2,019,061,912,044,646 v3).

2.2 | Brain nuclei sampling

Coronal sections (60 μm) were obtained in a cryostat (Thermo Scientific) from Paxinos and Franklin's the Mouse Brain Atlas coordinates: Bregma 1.10 to 0.74 for cingulate cortex (Cg) and corpus callosum (CC), Bregma -0.58 to 0.94 for hypothalamic paraventricular nucleus (PVN), and Bregma -1.46 to -2.06 for hippocampal regions Cornu Ammonis 1 (CA1), Cornu Ammonis 3 (CA3), Dentate Gyrus (DG) and amygdala (Amy).²⁴ Then, 0.8 and 1 mm diameter micropunches were obtained with sample corers (Fine Science Tools), and placed in dry ice frozen 1.5 ml tubes. Tubes were stored at -80°C until further processing. Additionally, 12 μm sections were obtained in the same first and third coordinate ranges and mounted onto SuperFrostPlus glass slides (Thermo Scientific), airdried, and stored at -20°C until further processing.

2.3 | RNA extraction and PCR

Total RNA was extracted from micropunches using TriPure isolation reagent (Merck), following the manufacturer's protocol. First strand cDNA was synthesized with M-MLV RT system (Promega), to 1 ng/ μl cDNA final concentration. qPCR reactions were run with iQ SYBR Green Supermix (Bio-Rad) in real-time PCR detection system (Bio-Rad). Expression levels were normalized to reference gene Rn18s. QuantiTect Primer Assays were purveyed by Qiagen. All information about primers used is contained in Table S1. All primer pairs were exon spanning and had amplification efficacies of $>90\%$.

2.4 | Immunohistochemistry and cell counting

Glass slides containing 12 μm coronal sections were air dried for 30 min. They were then immersed in PBS (Fresenius Kabi)-formalin (Sigma-Aldrich) 10% v/v solution, for 10 min, washed three times with PBS and blocked with PBS-Na₂CO₃ (Merck) 0.1% w/v-H₂O₂ (Supelco) 0.02% v/v for 10 min and washed again twice with PBS. After this, they were immersed in PBST (PBS-Tween 20 [Merck] 0.1% v/v), and blocked in PBST-BSA (Sigma-Aldrich) 5% w/v for 30 min. Slides were incubated with antibodies solution (Anti-NeuN [ab104225] 1:500, Abcam; RRID:AB_10711153) overnight at 4°C. After washing three times with PBST, they were incubated in secondary antibody mix (Rabbit EnVision; Dako) +5% normal mouse serum (Dako) for 30 min at room temperature, and then washed three times with PBST. Sections were then stained with liquid DAB+ substrate chromogen system (Dako) for 1 min and washed with deionized water, and counterstained with Mayer's hemalum (Sigma-Aldrich) solution 1:4 for 45 s. Finally, they were dried in hot air and slip covered. Digital images from Corpus Callosum were obtained as described in Amaya et al.²³ Images were processed with FIJI software (<http://fiji.sc>, RRID:

SCR_002285). From each image, blue channel was used to display immunopositive signal. Cingulate cingulum was parcellated in each image, and immunopositive cell bodies within were counted manually.

2.5 | Wes protein quantification

Blocks containing forebrain cortex, dorsal hippocampus and amygdala were dissected from brains using a mouse brain matrix (Zivic Instruments). Then, 1 mm slices were cut in Paxinos and Franklin's Mouse Brain Atlas²⁴ coordinates bregma 1.10–0.10 and bregma –1.22 to 2.18 approximately. Blocks were homogenized in Pierce radioimmunoprecipitation assay buffer (Thermo Scientific), and protein concentrations were measured using Pierce bicinchoninic acid protein assay kit (Thermo Scientific), and adjusted to 0.8 µg/µl. An automated western assay was then performed, using 12–230 kDa separation module (Protein Simple), in a WES system (Protein Simple), following protocol from manufacturer, using antibodies for GR (no. 3660, 1:20; Cell Signaling Technology; RRID:AB_11179215), MR (monoclonal antibody kindly provided by Professor Gomez-Sanchez,²⁵ clone1D5, 1:10), and glyceraldehyde 3-phosphate dehydrogenase (no. 5174, 1:20; Cell Signaling Technologies; RRID:AB_10622025). The image was analysed in Compass for Simple Western software (Protein Simple).

2.6 | Single cell data resources, metrics, and processing

The single cell data is based on the 10× scRNA-seq dataset published by the Allen Institute for Brain Science and publicly available at <https://portal.brain-map.org/atlas-and-data/rnaseq/mouse-whole-cortex-and-hippocampus-10x>. The data was clustered, and cluster names were assigned based on the Allen Institute proposal for cell type nomenclature (<https://portal.brain-map.org/explore/classes/nomenclature>). The topology of the taxonomy allowed to define regions of interest, cell classes (glutamatergic, GABAergic, or non-neuronal) and subclasses.^{26,27} The metadata was used to subset cells of the hippocampus region from the gene expression matrix. The newly obtained matrix was processed and analysed in R v3.6.1 according to the Seurat v3.1.5 pipeline for quality control, analysis, and exploration of scRNA-seq data²⁸ as described elsewhere.²⁹

2.7 | Statistical analysis

A Shapiro–Wilk test was applied to data subsets from qPCR and IHC assays, and 92% of all data subsets passed. Subsets were then compared by means of two-way ANOVA, with sex and genotype as factors. Tukey's multiple comparisons test was used as post-hoc analysis. Normalized data from WES assays were compared by means of Student's *t*-test. Significance level was set as $p < .05$. Testing was

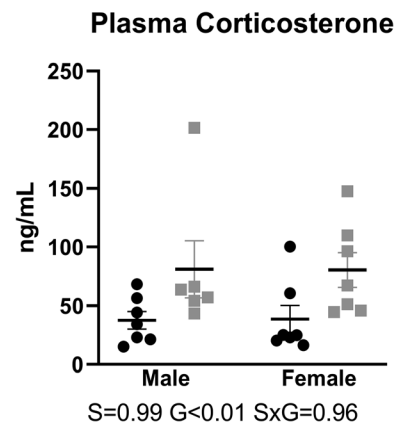


FIGURE 1 Basal plasma corticosterone at the moment of sacrifice, of wild-type and AdKO_{2.0} mice, measured by ELISA. Measurements were compared with two-way ANOVA. Black dots: wild-type; grey squares: AdKO_{2.0}

performed using GraphPad Prism 9 for Windows 64-Bit, version 9.0.1 (151) (GraphPad Software; RRID:SCR_002798).

3 | RESULTS

3.1 | Basal plasma corticosterone

Morning plasma corticosterone levels in 8–10-week-old mice were 37.6 ± 7.5 and 81.1 ± 24.3 ng/ml (mean \pm SEM), in WT ($n = 7$) and AdKO_{2.0} ($n = 6$) males, respectively and 38.6 ± 11.7 versus 80.5 ± 14.7 ng/ml (mean \pm SEM) in WT ($n = 7$) and AdKO_{2.0} ($n = 7$) females, respectively. A significant genotype effect was found ($p < .01$), indicating higher levels in AdKO_{2.0} mice compared to wild-type (Figure 1).

3.2 | Gene expression overviews

Allen Brain Atlas derived basal expression of all measured genes is depicted in Figure 2 to illustrate the extent of their cell type specific expression in male and female mouse hippocampus.²⁶ Table 1 summarizes graphically all significant gene expression changes observed in AdKO_{2.0} (Factor: Genotype), male (Factor: Sex), or male AdKO_{2.0} mice (Factor: Interaction). The complete mRNA expression dataset is shown in Supporting Information figures, while for readability, selected panels are shown in the individual figures in the main text. Although the total number of sacrificed animals was 28 ($n = 7$, for each of four groups: male wild-type, male AdKO_{2.0}, female wild-type, and female AdKO_{2.0}), different numbers of samples were lost in the dissection stage. Comparisons of gene expression in the different brain areas, and of immunohistochemical labelling were made with the respective number of remaining samples for every case.

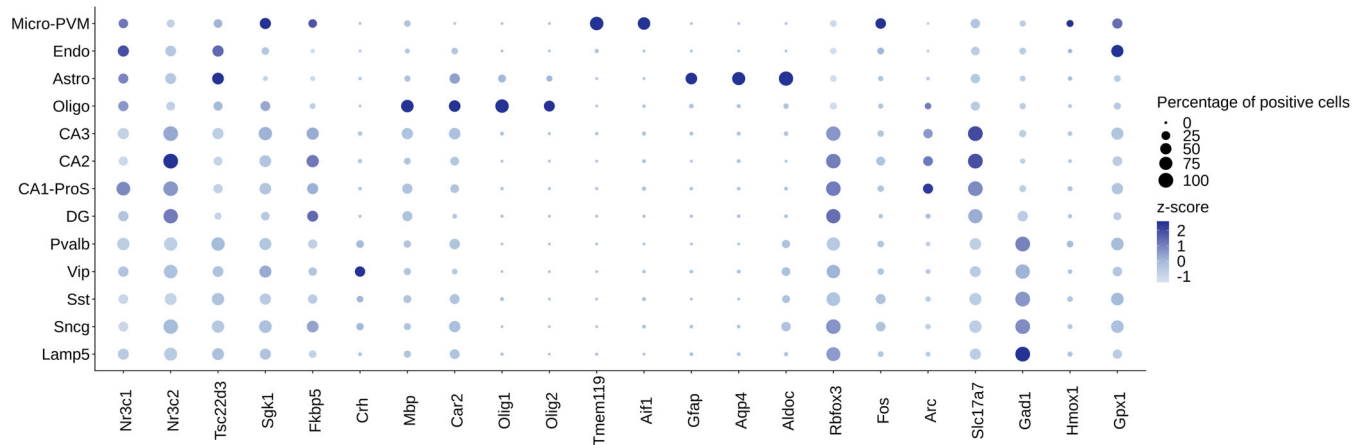


FIGURE 2 Normalized expression of measured genes in hippocampal cells under basal conditions. The dots represent gene centered log-normalized average expression (z-score) as colour and the percentage of positive cells as dot size. Micro-PVM: microglia-perivascular macrophages; Endo: endothelial cells; Astro: astrocytes; Oligo: oligodendrocytes; CA3, CA2, CA1-ProS and DG: glutamatergic neurons from Cornu Ammonis areas 3, 2, 1 and dentate gyrus, respectively; Pvalb, Vip, Sst, Sncg and Lamp5: GABAergic neurons expressing parvalbumin, vasoactive intestinal peptide, somatostatin, gamma-synuclein, or lysosome-associated membrane glycoprotein 5, respectively

TABLE 1 Overview of significant gene expression changes

Factor	Gene class	Cg	CC	PVN	CA1	CA3	DG	Amy	
Genotype	GR Targets	<i>Fkbp5</i> ↑	<i>Fkbp5</i> ↑	<i>Fkbp5</i> ↑	<i>Fkbp5</i> ↑	<i>Fkbp5</i> ↑	<i>Fkbp5</i> ↑	<i>Fkbp5</i> ↑	
			<i>Sgk1</i> ↑						
			<i>Tsc22d3</i> ↑						
				<i>Crh</i> ↓	<i>Crh</i> ↑			<i>Crh</i> ↑	
	GR and MR	<i>Mr</i> ↓							
		<i>Gr</i> ↓					<i>Gr</i> ↓		
	Oligodendrocytes		<i>Mbp</i> ↓	<i>Mbp</i> ↓					
			<i>Car2</i> ↓	<i>Car2</i> ↓	<i>Car2</i> ↓	<i>Car2</i> ↓		<i>Car2</i> ↓	
	Astrocytes					<i>Gfap</i> ↓			
			<i>Aqp4</i> ↓	<i>Aqp4</i> ↓		<i>Aqp4</i> ↓	<i>Aqp4</i> ↓	<i>Aqp4</i> ↓	<i>Aqp4</i> ↓
				<i>Aldoc</i> ↑		<i>Aldoc</i> ↑	<i>Aldoc</i> ↑	<i>Aldoc</i> ↑	
	Microglia		<i>Aif1</i> ↓		<i>Aif1</i> ↓	<i>Aif1</i> ↓		<i>Aif1</i> ↓	
	Neurons			<i>Rbfox3</i> ↑					<i>Rbfox3</i> ↑
			<i>Slc17a7</i> ↑						
			<i>Gad1</i> ↑						
Oxidative stress		<i>Hmox1</i> ↓		<i>Hmox1</i> ↓					
		<i>Gpx1</i> ↓							
Sex	Oligodendrocytes				<i>Mbp</i> ↓				
				<i>Car2</i> ↓					
							<i>Olig2</i> ↑		
	Microglia				<i>Tmem119</i> ↓				
	Neurons			<i>Aif1</i> ↓				<i>Fos</i> ↓	
Oxidative stress				<i>Fos</i> ↓	<i>Fos</i> ↓				
Interaction	GR					<i>Gr</i> ↓			
	Astrocytes						<i>Aqp4</i> ↓		
	Microglia				<i>Aif1</i> ↓				
	Neurons						<i>Gad</i> ↑		
	Oxidative stress					<i>Fos</i> ↓	<i>Arc</i> ↓	<i>Fos</i> ↓	
						<i>Nfe2l2</i> ↓			

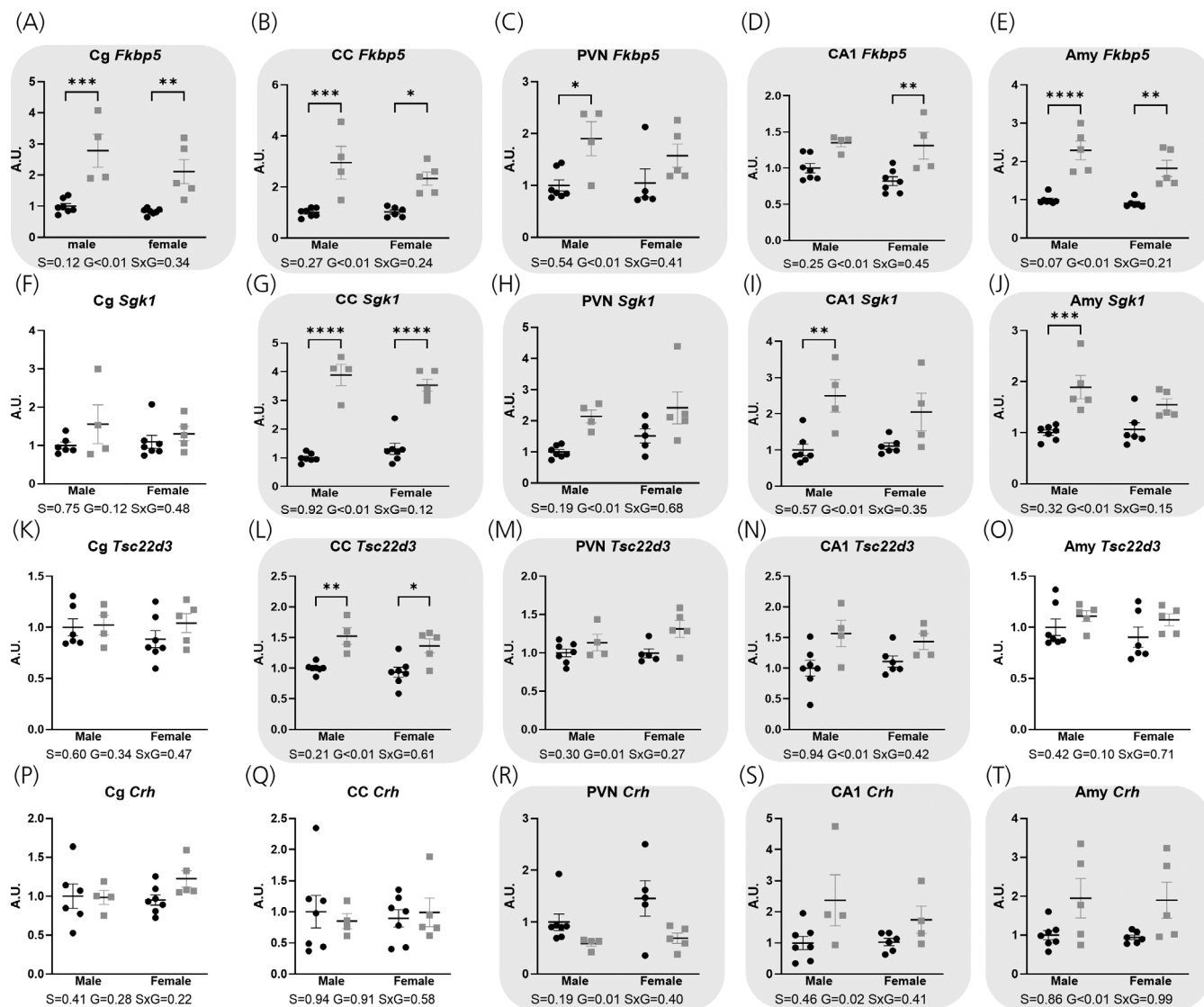


FIGURE 3 Expression of known GR targets (A–D: *Fkbp5*; F–G: *Sgk1*; K–O: *Tsc22d3*; P–T: *Crh*) in selected brain regions of wild-type and AdKO_{2.0} mice. qPCR data were compared with 2-way ANOVA. Black dots: wild-type; grey squares: AdKO_{2.0}. Amy, amygdala; A.U., arbitrary units; CA1, hippocampal cornu ammonis area 1; CC, corpus callosum; Cg, cingulate cortex; PVN, hypothalamic paraventricular nucleus. Significant effects ($p < .05$) are highlighted: S, sex (dashed frame); G, genotype (grey shade); SxG, interaction (dotted frame). Asterisks indicate significant Tukey's multiple comparisons test: * $p < .05$; ** $p < .01$; *** $p < .001$; **** $p < .0001$

3.3 | Glucocorticoid target genes

GR activation was tested by measuring the mRNAs coded by *Fkbp5*, *Sgk1*, *Tsc22d3* (commonly referred to as *Gilz*), and *Crh*. *Fkbp5* mRNA expression showed significant genotype effects with $p < .01$ in all brain regions (Figures 3A–E). Except for the cingulate cortex, significant genotype effects ($p < .01$ in all cases) were also found for *Sgk1* mRNA (Figures 3G–J). For *Tsc22d3* mRNA, significant genotype effects were found in CC ($p < .01$), PVN ($p = .01$), CA1 ($p < .01$) (Figure 3L–N), CA3 ($p = .01$) and DG ($p < .01$) (Figure S1S, T). For these three genes, increased expression in AdKO_{2.0} mice, compared to wild-type, was evident for all significantly affected regions. In the case of *Crh* mRNA, significant genotype effects were found only in PVN ($p = .01$) showing lower expression in AdKO_{2.0}

mice; and in CA1 ($p = 0.02$) and Amy ($p < .01$), in which higher expressions were observed in the AdKO_{2.0} mice (Figures 3R–T), compared to wild-type. This differential regulation by glucocorticoids is in agreement with previously published literature.³⁰ Together, these data confirm long lasting responsiveness of known GR target genes to the long-term glucocorticoid overexposure in AdKO_{2.0} mice.

3.4 | Mineralocorticoid and glucocorticoid receptors

Expression of mRNA for mineralocorticoid and glucocorticoid receptors (*Nr3c2* and *Nr3c1*, respectively) was measured. Significant effects for

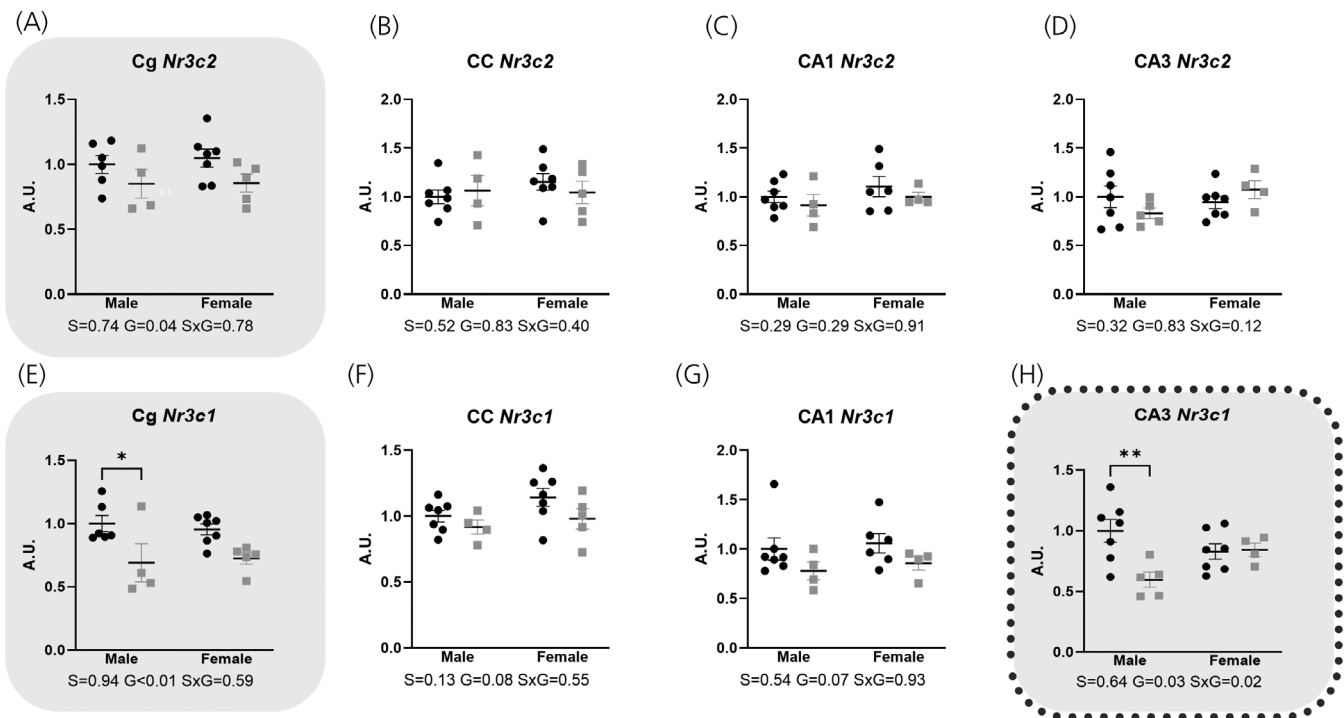


FIGURE 4 Expression of Nr3c2 (coding for MR, A–D) and Nr3c1 (coding for GR, E–H) in selected brain regions of wild-type and AdKO2.0 mice. qPCR data were compared with two-way ANOVA. Black dots: wild-type; grey squares: AdKO2.0. A.U., arbitrary units; CA1, hippocampal cornu ammonis area 1; CA3, hippocampal cornu ammonis area 3; CC, corpus callosum; Cg, cingulate cortex. Significant effects ($p < .05$) are highlighted: S, sex (dashed frame); G, genotype (grey shade); SxG, interaction (dotted frame). Asterisks indicate significant Tukey's multiple comparisons test p : * $< .05$; ** $< .01$

Nr3c2 mRNA were found only in Cg ($p = .04$), in which a decrease was observed in AdKO_{2.0} mice (Figure 4A), compared to wild-type. Nr3c1 mRNA expression in Cg ($p < .01$) and CA3 ($p = .03$) was found to be significantly decreased in AdKO_{2.0} mice as well (Figure 4E,H), with respect to wild-type. In CA3, the decrease was more pronounced in male AdKO_{2.0} mice ($p = .02$) (Figure 4H). The complete dataset regarding both receptors expression in all selected brain regions is displayed in Figure S2.

MR and GR protein was quantified in frontal cortex, hippocampus and amygdala from male mice. Normalized GR signal was significantly lower ($p = .04$) in AdKO_{2.0} mice in cortex only (Figure 5A–D). No significant differences were observed in MR assay (Figures 5E–H).

3.5 | Oligodendrocyte markers

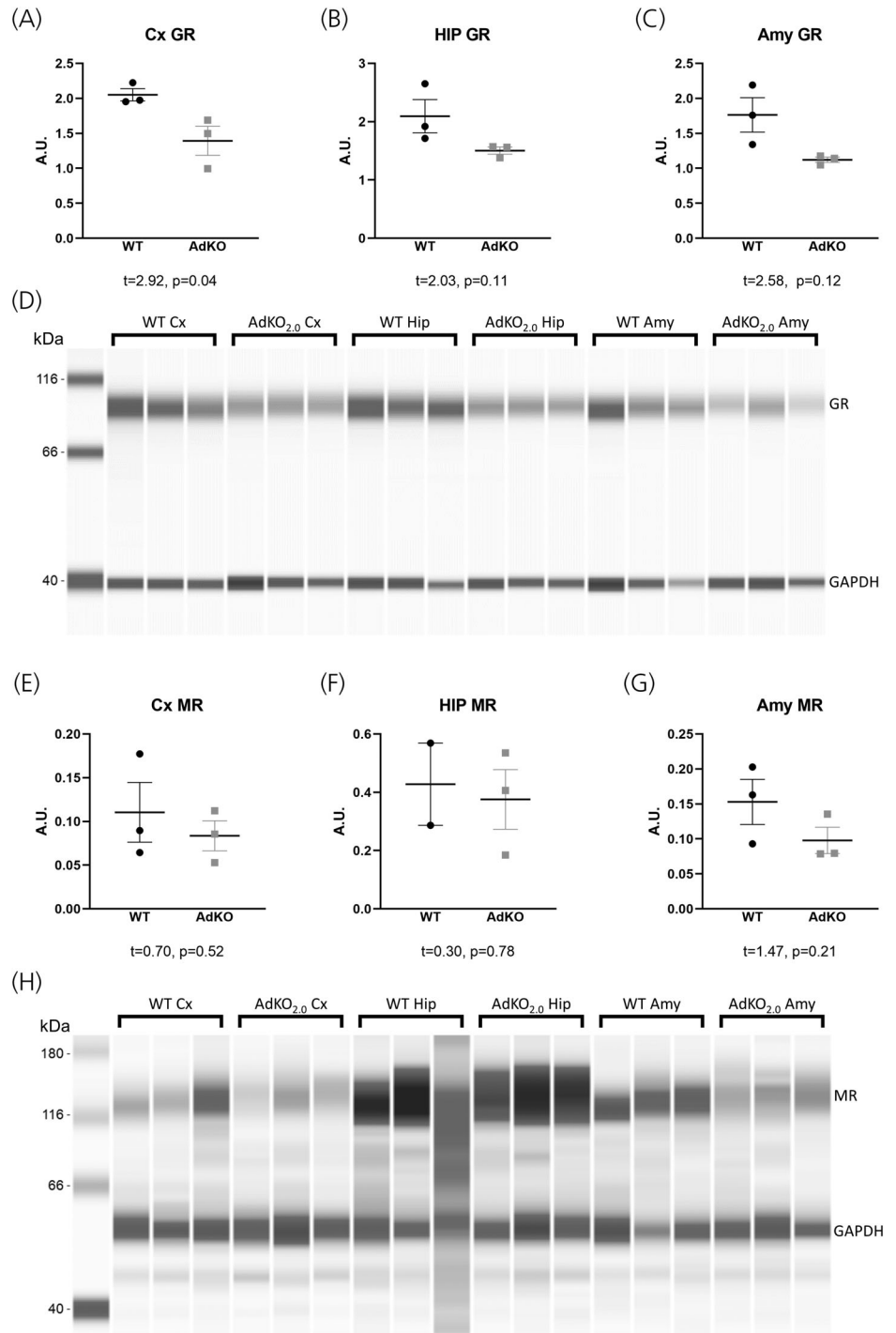
We earlier observed substantial changes in immunoreactivity of myelin basic protein (MBP),²³ primarily expressed in oligodendrocytes (Figure 2). At the mRNA level, we evaluated effects on mature oligodendrocytes by measuring expression of two genes that are predominantly expressed in these cells: *Mbp* and *Car2*. In the case of *Mbp*, significant genotype effects were found in CC ($p = .04$) (Figure 5A), and PVN ($p = .01$) (Figure S3C), indicating that AdKO_{2.0} mice presented an expression lower than wild-type. For *Car2*, significant genotype effects were found in CC ($p = .01$), CA1 ($p = .02$) (Figures 6D,E),

as well as in Cg ($p = .01$) (Figure S3H), PVN ($p < .01$) (Figure S3J), and Amy ($p < .01$) (Figure S3N); all describing decreased expression in AdKO_{2.0} mice in relation to wild-type. Possible effects on oligodendrocyte precursors were explored by measuring expression of *Olig1* and *Olig2*. There were no significant effects in either marker (Figures 6G–L), except for a sex effect in *Olig2* expressed in DG ($p = .03$), which pointed to a lower expression in females (Figure S3A), compared to males. In CA1 we found a significant sex effect in *Mbp* expression ($p = .03$), suggesting expression in female higher than in male mice (Figure 6B). Together these findings suggest that long term glucocorticoid exposure does not affect the pool of oligodendrocyte precursors but does substantially affect mature oligodendrocyte turnover or rather (given that the markers did not consistently cofluctuate) function.

3.6 | Astrocyte markers

In our previous work we found strongly suppressed immunoreactivity of the astrocyte marker GFAP,²³ often used to detect reactive astrocytes. Here were evaluated by measuring expression of *Gfap*, *Aqp4*, and *Aldoc*, three genes with highly specific expression in astrocytes (Figure 2). In the expression of *Gfap* a significant genotype effect ($p = .02$) was found only in CA1, which indicated a decrease in AdKO_{2.0} mice, compared to wild-type (Figure 7B).

FIGURE 5 Expression of GR (coded by Nr3c1, A–C) and MR (coded by Nr3c2, E–G) in selected brain regions of wild-type and AdKO2.0 mice. WES data were compared with Student's t-test. D and H show capillary electrophoresis images of GR and MR, respectively



Aqp4 and *Aldoc* are expressed specifically in astrocytes (Figure 2). For *Aqp4* expression, significant genotype effects were obtained in CC ($p < .01$), CA1 ($p = .02$), CA3 ($p = .01$) (Figures 7D–F), Cg ($p = .02$), DG ($p = .01$) and Amy ($p = .02$) (Figure S4H,M,N); in all of them AdKO_{2.0} mice showed a decrease in mRNA level with respect to wild-type. Additionally, a significant factor interaction was also found in *Aqp4* expression in DG ($p = .03$), with AdKO_{2.0} male group showing the lowest values of all groups (Figure S4M). *Aldoc* mRNA expression showed significant genotype effects in CC, CA1, CA3 ($p < .01$ in each) (Figure 7G–I), and DG ($p = .01$) (Figure S4T); in all cases with higher levels in AdKO_{2.0} mice, compared to wild-type. Together these data

suggest that astrocyte function is substantially affected by chronic glucocorticoid overexposure. They do not allow firm conclusions as to the nature of these changes, given that two generically expressed genes are regulated in opposite directions; however, *Aqp4* mRNA has been established earlier as a GR target.³¹

3.7 | Microglia markers

We earlier found that Iba1 immunoreactivity was strongly suppressed in AdKO_{2.0} mice.²³ Here, microglia were assessed by

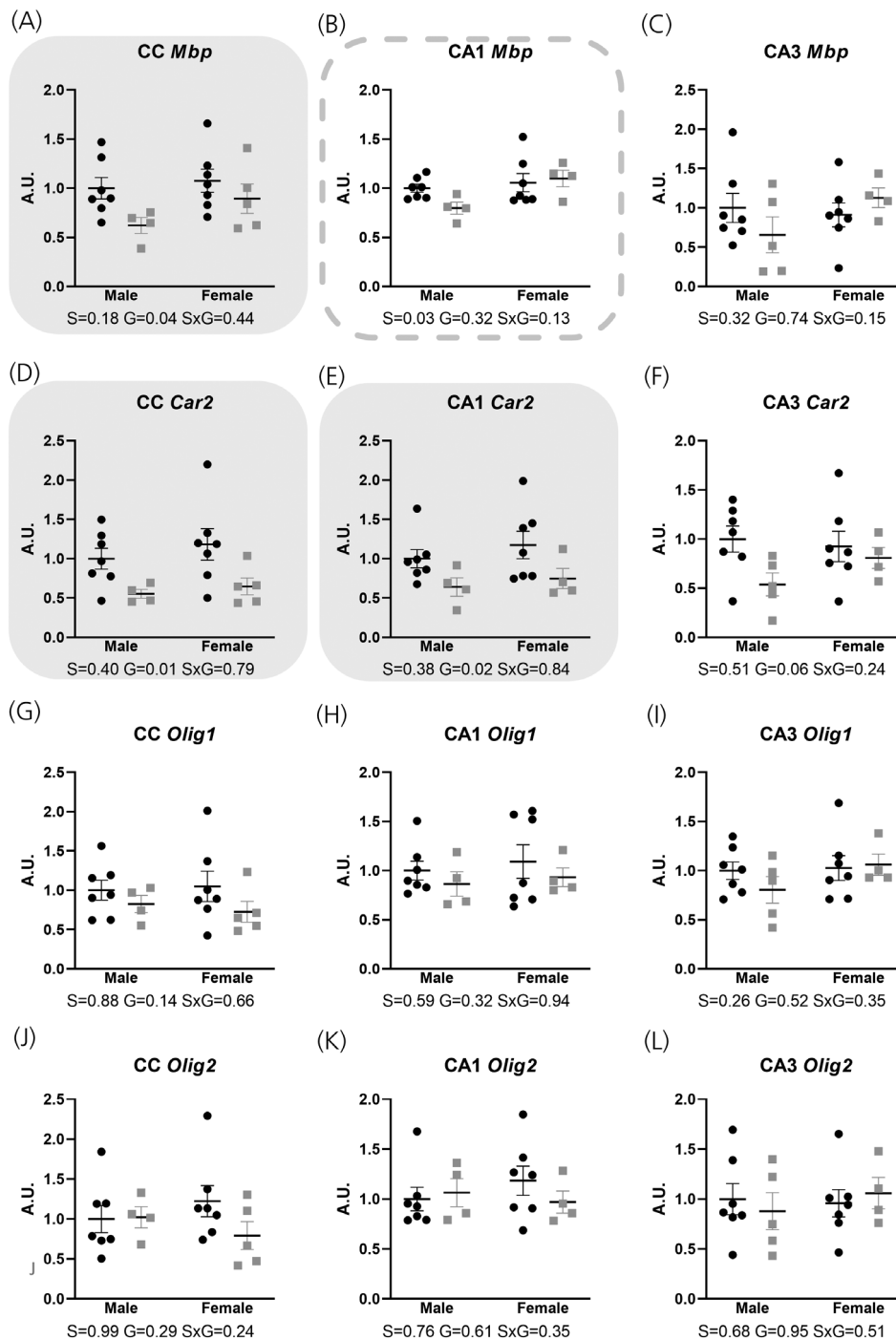


FIGURE 6 Expression of mature oligodendrocyte (A–C: Mbp; D–F: Car2) and oligodendrocyte precursor (G–I: Olig1; J–L: Olig2) marker genes in selected brain regions of wild-type and AdKO_{2.0} mice. qPCR data were compared with two-way ANOVA. Black dots: wild-type; grey squares: AdKO_{2.0}. A.U., arbitrary units; CA1, hippocampal cornu ammonis area 1; CA3, hippocampal cornu ammonis area 3; CC, corpus callosum. Significant effects ($p < .05$) are highlighted: S, sex (dashed frame); G, genotype (grey shade); SxG, interaction (dotted frame)

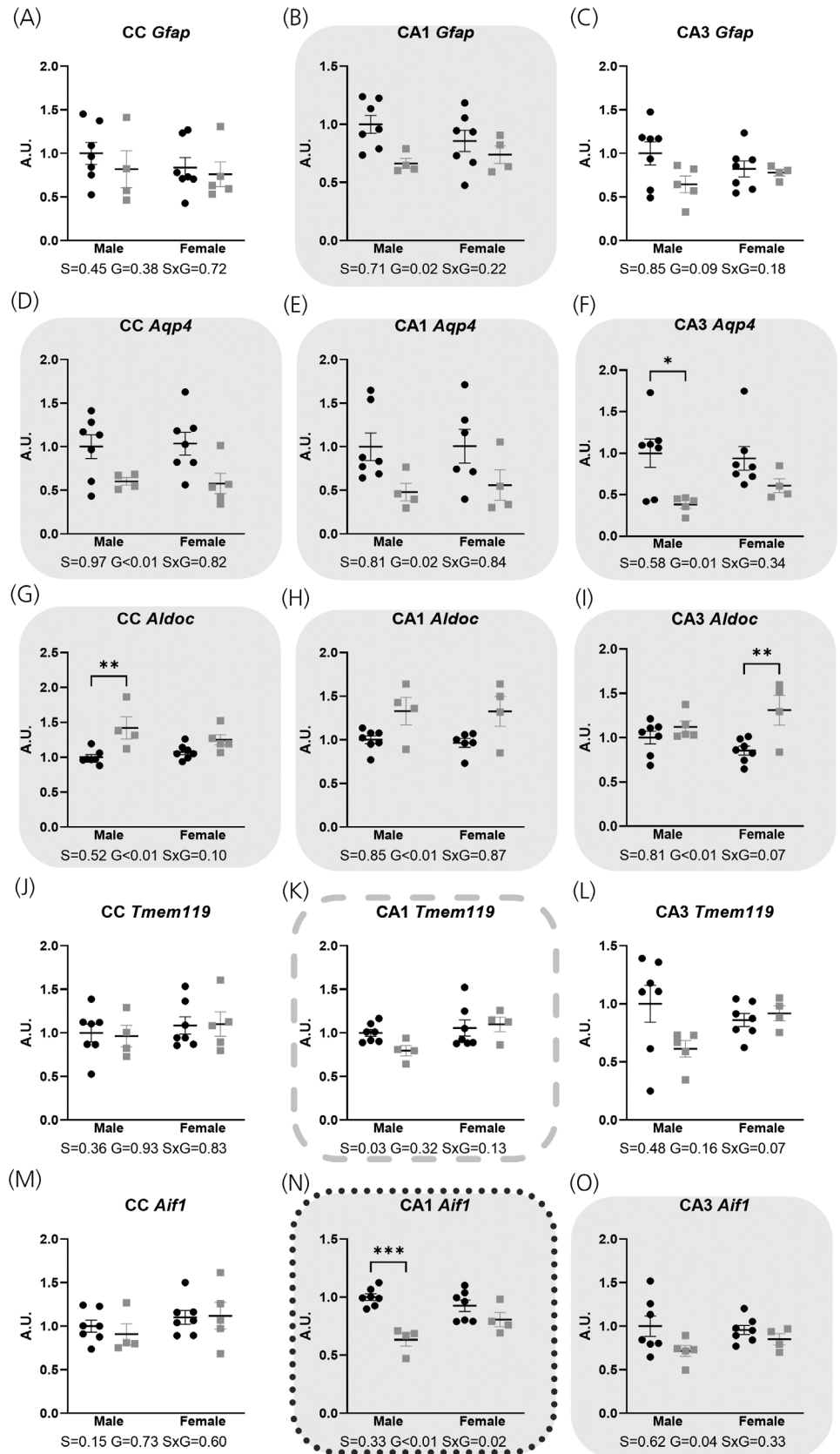
measuring expression of the *Tmem119* as a marker for total microglia content, and *Aif1* (coding for IBA1 protein) as a marker for reactive microglia. Except for a sex effect found in CA1 ($p = .03$) (Figure 7K), *Tmem119* expression showed no significant changes. In the case of *Aif1* expression, significant genotype effects were observed in CA1 ($p < .01$), CA3 ($p = .04$) (Figure 7N,O), Cg ($p < .01$), PVN ($p < .01$) and Amy ($p < .01$) (Figure S5H,J,N), all suggesting that AdKO_{2.0} mice presented a lower expression than wild-type; additionally, a significant sex effect was found in PVN ($p = .02$) indicating lower expression in males compared to females (Figure S5J); and a significant factor interaction effect was found in

CA1 ($p = .02$) (Figure 7N), which shows male AdKO_{2.0} mice to have the lowest expression of all groups. The fact that the marker for total microglia was unchanged, contrary to the case of the marker for reactive astroglia, suggests that the activation status, but not the number, of microglia cells was affected in AdKO_{2.0} mice.

3.8 | Neuronal markers

Neuronal populations were investigated by measuring *Rbfox3* (coding for NeuN protein), the glutamatergic neuron specific gene *Slc17a7*,

FIGURE 7 Expression of astrocytic (A–C: *Gfap*; D–F: *Aqp4*; G–I: *Aldoc*) and microglial (J–L: *Tmem119*; M–O: *Aif1*) markers in selected brain regions of wild-type and AdKO2.0 mice. qPCR data were compared with 2-way ANOVA. Black dots: wild-type; grey squares: AdKO2.0. A.U., arbitrary units; CA1, hippocampal cornu ammonis area 1; CA3, hippocampal cornu ammonis area 3; CC, corpus callosum. Significant effects ($p < .05$) are highlighted: S, sex (dashed frame); G, genotype (grey shade); SxG, interaction (dotted frame). Asterisks indicate significant Tukey's multiple comparison test $p: * < .05$; $** < .01$; $*** < .001$



and the GABA-ergic neuron specific gene *Gad1*. For *Rbfox3*, significant genotype effects were found in the CC ($p = .02$) and Amy ($p = .03$) (Figures 8B,D) in both cases pointing to an expression in

AdKO_{2.0} mice higher than wild-type. *Slc17a7* was found to be significantly lower in AdKO_{2.0} mice ($p = .046$) in the Cg, compared to wild-type (Figure 8E). Both *Slc17a7* and *Gad1* mRNA expressions were

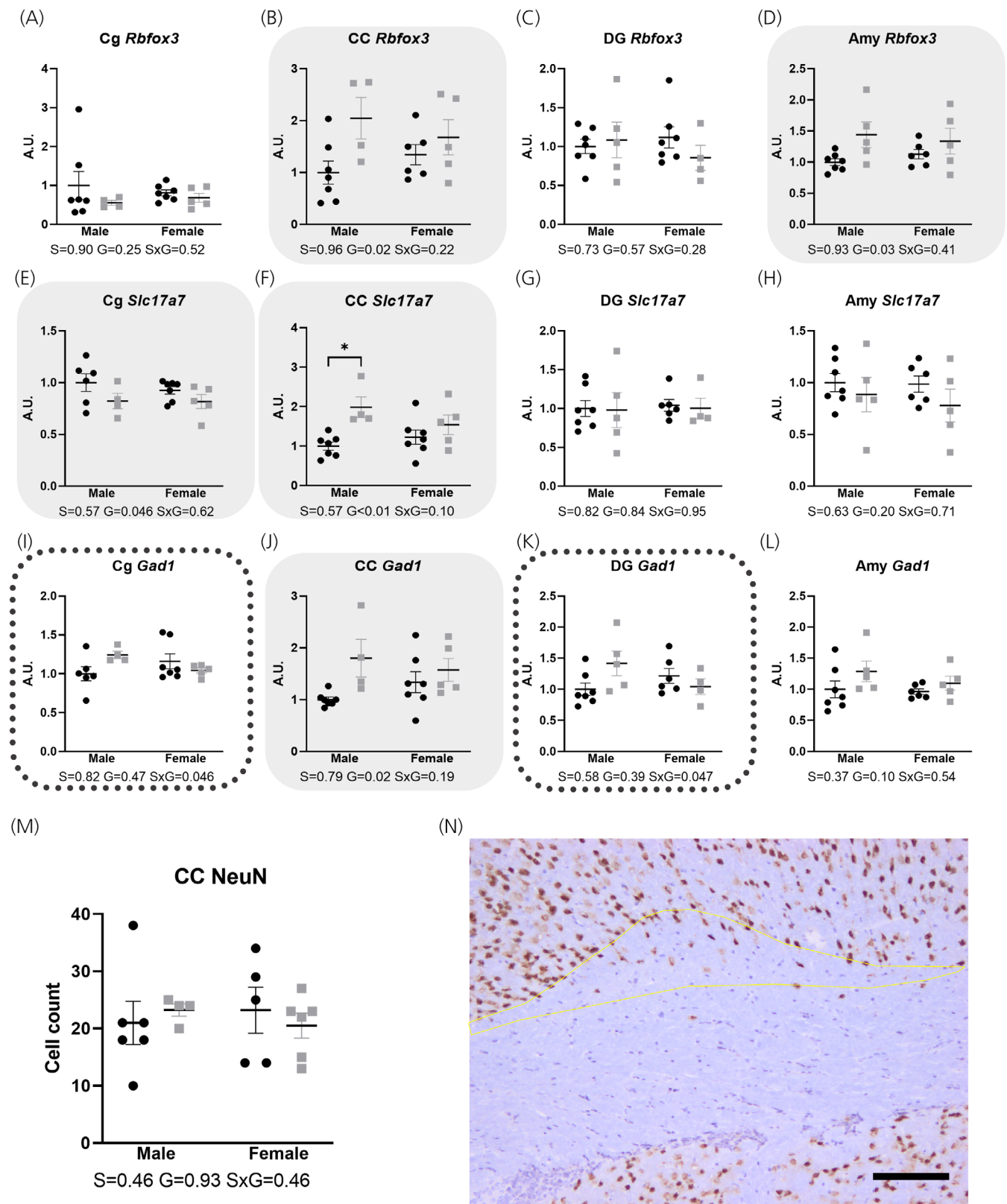
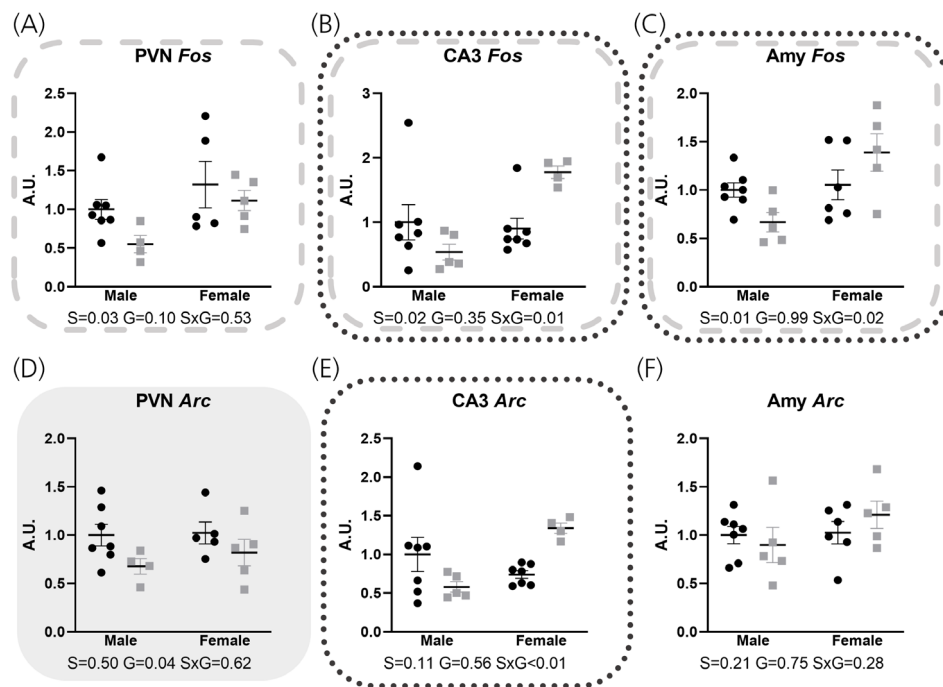


FIGURE 8 Expression of neuron associated genes (A–D: *Rbfox3*; E–H: *Slc17a7*; I–L: *Gad1*); and quantification of immunopositive cell bodies for NeuN (M) in selected brain regions of wild-type and AdKO2.0 mice. Panel N depicts NeuN immunohistochemical staining in the CC and surroundings; yellow highlight indicates parcellation of the cingulum subsection of the CC that was used for cell count; Black bar = 100 μ m. qPCR and immunopositive cell count data were compared with two-way ANOVA. Black dots: wild-type; grey squares: AdKO2.0. Amy, amygdala; A.U., arbitrary units; CC, corpus callosum; Cg, cingulate cortex; DG, hippocampal dentate gyrus. Significant effects ($p < .05$) are highlighted: S, sex (dashed frame); G, genotype (grey shade); SxG, interaction (dotted frame)

FIGURE 9 Expression of cellular activity associated genes (A–C: *Fos*; D–F: *Arc*) in selected brain regions of wild-type and AdKO2.0 mice. qPCR data were compared with two-way ANOVA. Black dots: wild-type; grey squares: AdKO2.0. Amy, amygdala; A.U., arbitrary units; CA3, hippocampal cornu ammonis area 3; PVN, hypothalamic paraventricular nucleus. Significant effects ($p < .05$) are highlighted: S, sex (dashed frame); G, genotype (grey shade); SxG, interaction (dotted frame)



found to be significantly higher in AdKO_{2.0} mice, with relation to wild-type, in CC ($p < .01$ and $p = .02$, respectively) (Figure 8F,J). Also, *Gad1* was significantly higher in AdKO_{2.0} male mice in Cg (0.046) and DG ($p = .047$) in comparison to wild-type (Figures 8I,K). The complete dataset of the expression of the three referred markers in all brain regions is displayed in Figure S6A–U.

Based on the surprising presence of the neuronal marker NeuN in punches of corpus callosum, and the concurrent increase in *Gad1* mRNA, we stained sections with NeuN antibody, in order to check for the presence of neuronal (probably GABA-ergic) cells in this white matter area (Figures 8M,N). We observed presence of NeuN positive cells in the cingulate cingulum, but these were not more abundant in AdKO_{2.0} mice than in wild-type. We concluded that there the increased mRNA expression may be related to GABA-ergic neurons adjacent to the corpus callosum, which may have been included in the micropunches during dissection. However, for lack of sampling that is compatible with stereological measurements, we were unable to further substantiate this notion. We conclude that there are no major changes in terms of markers for the two main neuronal subdivision, GABA-ergic and glutamatergic cells, although some of the observed mRNA changes may be subject to future studies.

3.9 | Cellular activity

Basal cellular activity was assessed by measuring expression of immediate early genes *Fos* and *Arc*. Of note, while these genes are routinely interpreted as markers for neuronal activity, basal *Fos* mRNA expression was highest in oligodendrocytes in the Allen Brain Atlas data (Figure 2). Significant sex effects on *Fos* expression were found in PVN ($p = .03$), CA3 ($p = .02$) and Amy ($p = .01$)

(Figures 9A–C), all describing an increased expression in females compared to males; in addition, significant factor interactions were also found in CA3 ($p = .01$), and Amy ($p = .02$) (Figures 9B,C) indicating expression levels in female AdKO_{2.0} mice higher than the other groups. For *Arc* mRNA a significant genotype effect was found in PVN ($p = .04$) (Figure 9D), based on an expression in AdKO_{2.0} mice lower than wild-type, and a significant factor interaction was found in CA3 ($p < .01$) (Figure 9E) with AdKO_{2.0} male mice having the lowest expression of all groups. The complete dataset of the expression of both referred markers in all selected brain regions is displayed in Figures S6V–I'.

3.10 | Oxidative stress related genes

Because chronic administration of glucocorticoids is considered a risk factor for the viability of neuronal populations,^{32,33} markers for oxidative stress were explored by measuring expression of *Nfe2l2*, *Sod1*, *Hmox1*, *Gpx1* and *Cat* genes. *Nfe2l2* mRNA showed a significant sex effect in PVN ($p = .01$) (Figure S7C) in which expression in females is higher compared to males; and a significant factor interaction in CA3 ($p < .01$) (Figure S7E), in which AdKO_{2.0} males show lower levels than the rest of the groups. *Sod1* showed no significant effects. In the case of *Hmox1*, significant genotype effects were found in Cg ($p = .01$) and PVN ($p = .03$) (Figures 10A,B), both showing a decrease in AdKO_{2.0} mice in comparison to wild-type. For *Gpx1*, a significant genotype effect was found only in Cg ($p < .01$) (Figure 10D) which indicates a decrease of expression in AdKO_{2.0} mice, compared to wild-type. No significant effects were found in *Cat* expression. We concluded that there is no overt regulation of oxidative stress marker genes in AdKO_{2.0} mice.

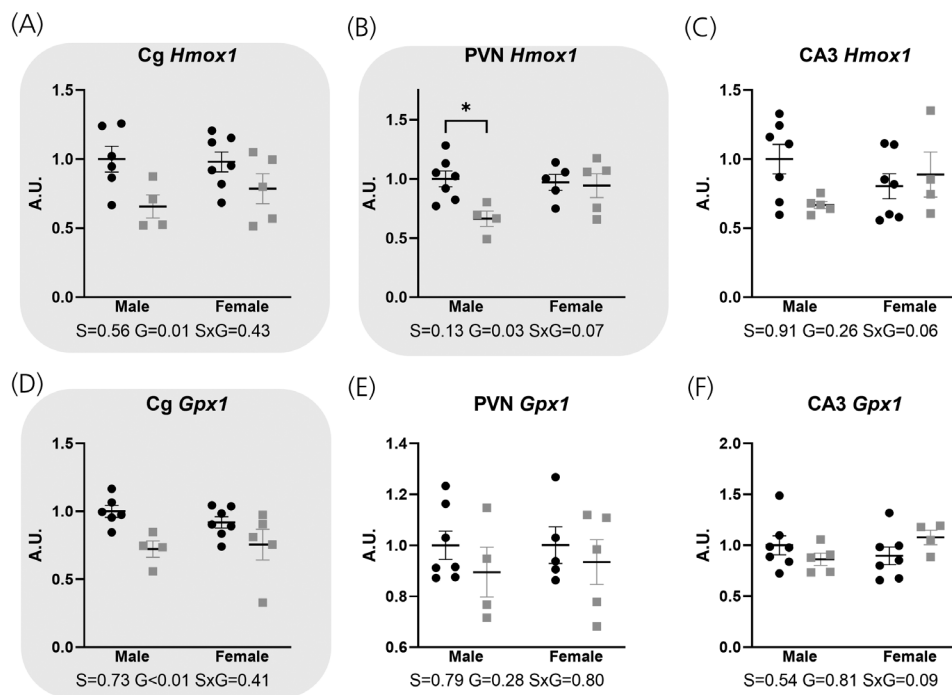


FIGURE 10 Expression of oxidative stress associated genes (A–C: Hmox1; D–F: Gpx1) in selected brain regions of wild-type and AdKO2.0 mice. qPCR data were compared with two-way ANOVA. Black dots: wild-type; grey squares: AdKO2.0. A.U., arbitrary units; CA3, hippocampal cornu ammonis area 3; Cg, cingulate cortex, PVN, hypothalamic paraventricular nucleus. Significant effects ($p < .05$) are highlighted: S, sex (dashed frame); G, genotype (grey shade); SxG, interaction (dotted frame)

4 | DISCUSSION

To better understand the consequences of chronic overexposure of the brain to endogenous glucocorticoids, we compared gene expression of known glucocorticoid target genes, and of a number of cellular markers genes between AdKO_{2.0} mice and wild-types. We found major differences on markers of all three glial cell types. While expression of the exclusively neuronal target gene *Crh* was affected, generic markers for GABA-ergic and glutamatergic neurons were largely spared. We did not observe consistent changes in genes linked to oxidative stress.

We used qPCR mRNA quantification in punches from seven brain regions. Although this approach provides less information than a transcriptomics approach per region, it allows for a more extensive analysis than what would be possible using antibodies. The use of mRNA measures as markers for cell populations comes with some caveats. First, protein levels and mRNA levels can differ—which is clearly the case for GR in our present data. Also, *Mbp* and *Gfap* in our previous immunostaining²³ showed much stronger differences between genotypes than our present mRNA data. Second, the markers may be affected by the phenotype, that is, regulated by glucocorticoids. This may lead to discrepant data for markers of a particular cell type, as is the case for astrocytes in this study. Third, the mRNA measurement is a bulk measurement. This perhaps makes the approach more vulnerable to false negative findings compared to immunohistochemical analysis. Nevertheless, our data allowed us to observe clear effects.

AdKO_{2.0} mice presented widespread increases in expression of *Fkbp5*, *Sgk1* and *Tsc22d3* (coding for GILZ), with some exceptions mainly in the cingulate cortex. The basal expression of the classical target genes varies among the different cell types in the hippocampus.

Accordingly, their increased expression probably reflects different cell types. Expression of *Crh* is restricted to neurons, and its bidirectional regulation in hypothalamus and amygdala areas is in line with known glucocorticoid effects.³⁰ We are unaware of previous data reporting *Crh* mRNA induction in the diffusely distributed CRH cells in the hippocampus. These results indicate that in our mice there is a strong, widespread and sustained transcriptional effects as a result of chronic hypercorticism, probably in all cell types of the brain. This is further substantiated by the strong downregulation of *Aqp4* in astrocytes.

Based on receptor affinities it is tempting to interpret the effects of chronically elevated corticosterone as mediated by GR rather than MR,¹ but our data do not allow to distinguish. For hippocampus, GR is the predominant receptor in oligodendrocytes and microglia (Figure 2). Also, CRH in the PVN is an established GR target gene. However, recent findings suggest that MR can be a mediator of elevated levels of corticosterone,^{34–36} and experiments using MR and GR antagonists will have to establish specific receptor involvement for most genes. GR mRNA was modestly suppressed, but our WES analysis suggests that homologous downregulation of GR is more extensive at the protein level – as the GR protein suppression in AdKO_{2.0} mice seems widespread, even if the experiment was not sufficiently powered to reach significance. Clearly, homologous downregulation of *Nr3c1*³⁷ does far from fully compensate for hormone exposure in the brain.

As markers for oligodendrocytes, we selected *Mbp*, *Car2*, *Olig1* and *Olig2* (Figure 2). Of these only *Olig1* was previously identified as glucocorticoid responsive.^{38,39} *Olig1* or *Olig2* mRNA expression was unchanged, suggesting that mobile, immature oligodendrocyte precursors might be resilient to chronic corticosterone overload.^{40–43} *Mbp* and *Car2* participate in myelination and myelin compaction in mature

oligodendrocytes.⁴⁴ Mbp mRNA expression was reduced in corpus callosum and PVN, but overall changes were much more modest than we earlier found using immune staining. Car2 mRNA, which is substantially enriched in oligodendrocytes, was significantly reduced in cingulate cortex, corpus callosum, hippocampal CA1 and amygdala. This result indicates that under chronic hypercorticotestosterone oligodendrocyte precursors might still be able to differentiate and migrate, but mature oligodendrocyte function is probably compromised. This is in concordance with widespread changes in white matter volumes that has been observed in the brains of these mice²³ and the changes in white matter integrity observed in Cushing's patients.^{19,45}

Tmem119 is expressed exclusively in microglia and its use as a general microglia marker is supported by the fact that is not affected by M1 or M2-type activation stage.⁴⁶ *Aif1* mRNA was not detected in hippocampus in basal conditions in the Allen Brain Atlas data, but its translational product *Iba1* is widely used as an indicator of microglial activation. We interpret the combined lack of effects on *Tmem119* mRNA and reduced *Aif1* mRNA levels as indicative of suppression of classical microglial activation mechanisms without an effect on overall microglia numbers. This is in line with our previous immunostainings,²³ and research by others that used exposure to chronic stress or chronic high levels of corticosterone, in basal conditions as well as in response to stroke.^{47–49} Also, in vitro exposure to corticosterone had strong suppressive effects on microglia.^{50,51} Thus, M1 type activation in microglia is probably suppressed due to chronic hypercorticotestosterone.

Previously we observed widespread reduction in GFAP immunoreactivity, but at mRNA we did not find robust changes. This coincides with the results in astrocyte cultures by Carter et al.,⁵² although some reports did find mRNA changes after glucocorticoid treatment.⁵³ The discrepancy between the current and our previous results²³ might arise from the fact that GFAP protein regulation can occur at the level of protein translation or turnover,^{54–57} or from a variation in the degree of GFAP protein incorporation to intermediate filament networks (which is the state usually targeted by primary antibodies).⁵⁸

AdKO_{2.0} mice presented a widespread decrease in *Aqp4* mRNA expression but increased *Aldoc* mRNA. We initially selected *Aqp4* as an astrocyte marker but it has been observed in other experiments that chronic unpredictable stress, methylprednisolone (in acute spinal cord injury paradigm) or dexamethasone, all decrease mRNA and protein expression in AQP4, in a GR dependent manner. Dexamethasone also abolishes polarization of AQP4 expression in astrocytes.^{31,59,60} As AQP4 is strongly linked to waste clearance from the brain via glymphatic flow, it is likely that this process is impaired in our mice, and perhaps also CS patients.³¹ It was also previously shown that exposure to corticosteroids increases *Aldoc* mRNA expression in astrocytes both in vitro and in vivo.^{52,53} Altogether, the present data confirm that astrocytic function is compromised under chronic circulating corticosteroid overload. In view of the large and consistent effects, it will be of interest to determine the functional consequences of these effects, for example, in cell-type specific knockout mice.⁶¹

AdKO_{2.0} mice showed a significant increase of *Rbfox3* mRNA expression in corpus callosum and amygdala. In corpus callosum we

also observed an increase in the expression of markers for GABAergic cells. However, since there were no significant differences in the amount of NeuN positive cell nuclei in the white matter areas, the increased *Rbfox3* mRNA signal may be due to the accidental inclusion of grey matter tissue surrounding the cingulum during dissection using the micropunch sample corers. Although we were not able to quantify NeuN immunostaining in amygdala, the increase in *Rbfox3* mRNA expression might be related to a larger amygdalar volume, as we have previously established in these mice.²³ Earlier work established that chronic stress or chronic corticosteroid administration can actually increase neuronal densities in certain areas of the brain, particularly in medial prefrontal cortex,⁶² although increase arborization after corticosterone treatment in the amygdala suggests additional mechanisms.⁶³ Decreased *Slc17a7* (Cg) and increased *Gad1* expression (CG and male dentate gyrus) in our data may indicate an increased inhibitory tone due to chronic exposure to corticosterone.

Although glucocorticoids may endanger particular cell types to excitotoxicity, AdKO_{2.0} mice presented significant decreases of oxidative stress markers *Hmox1* and *Gpx* mRNA expression in cingulate cortex and (for *Hmox1*) hypothalamic paraventricular nucleus. The lack of effects in most of the regions sampled suggest that the oxidative stress response machinery is spared from effects of chronic hypercorticotestosterone. "Endangerment" of neurons after corticosterone exposure may however become evident after additional challenges to the system, including age-related "wear and tear." However, in the relatively young mice used in this study we observed very limited evidence for increased vulnerability/exposure to oxidative stress.

Fos mRNA expression was significantly decreased in male mice in PVN, CA3 and amygdala. *c-FOS* is usually referred as an indicator of neuronal activation, but according to the available single cell RNA-seq data, it is a gene that is also strongly expressed in microglia under basal conditions. In fact, *Fos* expression can be upregulated by exposure to glutamate in microglia,⁶⁴ and it is required for microglial activation in response to noxious stimuli (e.g., LPS).⁶⁵ In the present study, it was not possible to discern if the *Fos* mRNA expression changes originate in neurons or microglia. The lower levels of immediate early gene expression in the PVN of AdKO_{2.0} mice may point to suppressive effects on corticosterone on the parvocellular CRH neurons as part of ongoing negative feedback.⁶⁶

In clinical populations, the great majority of Cushing's patients are women.⁶⁷ We obtained significant intrinsic sex effects as well as interactions between genotype and sex in genes related to oligodendrocytes, microglia, neuronal activity and oxidative stress. Most of these effects locate in PVN and hippocampus, where there is substantial coexpression of MR/GR with sex steroid receptors.²⁹ These differences were generally modest and restricted to single areas for each gene, with neuronal activation markers as the most consistently different between sexes. It has been shown that there are sexual differences in oligodendrocyte precursor proliferation and metabolism; microglial cell density, membrane properties and antigen presenting potential; and in both types of cells, gene expression profile.^{68,69} Long-term potentiation in hippocampal neurons is also sexually

dimorphic, and appears to be influenced by oestrous cycle hormonal fluctuations.⁷⁰ Finally, Nfe2l2 mRNA and protein levels are differentially regulated in male and female embryos exposed to oxidative stress.⁷¹ Although the extent of significant interactions between sex and genotype was modest in our data, compared to overall genotype effects, it will be of interest to study the role of gender and sex steroids in more detail in future studies, for example, with more comprehensive transcriptome analyses.

In conclusion, our data confirm and extend the notion that long-term exposure affects all major cell populations in the brain. In young adult mice this is not necessarily in terms of overall presence of cell markers, but certainly at the level of activation of, in particular, glial cell populations. Although the effects on Crh mRNA also suggest an immediate substrate for the emotional vulnerability in patients with Cushing's disease and glucocorticoid overexposure due to other causes, effects on many other signaling factors remain to be established. It will be also of interest to study to what extent the observed effects respond to normalization of corticosterone exposure, or treatment with GR antagonists, both current options for treatment of Cushing's syndrome.

ACKNOWLEDGEMENTS

We would like to thank Dr Elly Hol for discussion of our data, and Dr Elise P. Gomez-Sanchez for kindly providing MR monoclonal antibodies. This work was supported by CONACyT (grant number 440584) and Agence Nationale pour la Recherche (grant numbers ANR-14-CE12-0007-01 and ANR-18-CE14-0012-02).

CONFLICT OF INTEREST

OCM collaborates with, and receives funding from, Corcept Therapeutics who develop GR antagonists for a variety of indications related to hypercorticism.

AUTHOR CONTRIBUTIONS

Eva Myriam Goussivi Viho: Data curation; resources. **Hetty C. M. Sips:** Data curation; investigation; methodology. **Reshma A. Lalai:** Investigation; methodology. **Isabelle Sahut-Barnola:** Methodology; resources. **Typhanie Dumontet:** Methodology; resources. **Nathanaelle Montanier:** Methodology; resources. **Alberto M. Pereira:** Writing – review and editing. **Antoine Martinez:** Conceptualization; funding acquisition; project administration; resources; supervision; writing – review and editing.

PEER REVIEW

The peer review history for this article is available at <https://publons.com/publon/10.1111/jne.13125>.

DATA AVAILABILITY STATEMENT

The data that support the findings of this study are available from the corresponding author upon reasonable request.

ORCID

Jorge Miguel Amaya  <https://orcid.org/0000-0002-5382-5183>

Eva M. G. Viho  <https://orcid.org/0000-0002-1505-6598>

Typhanie Dumontet  <https://orcid.org/0000-0002-1328-9515>

Nathanaelle Montanier  <https://orcid.org/0000-0003-2748-5610>

Alberto M. Pereira  <https://orcid.org/0000-0002-1194-9866>

Antoine Martinez  <https://orcid.org/0000-0001-9304-5061>

Onno C. Meijer  <https://orcid.org/0000-0002-8394-6859>

REFERENCES

1. Reul JM, de Kloet ER. Two receptor systems for corticosterone in rat brain: microdistribution and differential occupation. *Endocrinology*. 1985;117(6):2505-2511.
2. Patel PD, Lopez JF, Lyons DM, Burke S, Wallace M, Schatzberg AF. Glucocorticoid and mineralocorticoid receptor mRNA expression in squirrel monkey brain. *J Psychiatr Res*. 2000;34(6):383-392.
3. Cao-Lei L, Suwansirikul S, Jutavijittum P, Meriaux SB, Turner JD, Muller CP. Glucocorticoid receptor gene expression and promoter CpG modifications throughout the human brain. *J Psychiatr Res*. 2013;47(11):1597-1607.
4. Perlman WR, Webster MJ, Herman MM, Kleinman JE, Weickert CS. Age-related differences in glucocorticoid receptor mRNA levels in the human brain. *Neurobiol Aging*. 2007;28(3):447-458.
5. Alt SR, Turner JD, Klok MD, et al. Differential expression of glucocorticoid receptor transcripts in major depressive disorder is not epigenetically programmed. *Psychoneuroendocrinology*. 2010;35(4):544-556.
6. Harnett NG, van Rooij SJH, Ely TD, et al. Prognostic neuroimaging biomarkers of trauma-related psychopathology: resting-state fMRI shortly after trauma predicts future PTSD and depression symptoms in the AURORA study. *Neuropsychopharmacology*. 2021;46:1263-1271.
7. de Kloet ER, Joels M, Holsboer F. Stress and the brain: from adaptation to disease. *Nat Rev Neurosci*. 2005;6(6):463-475.
8. Nieman LK. Cushing's syndrome: update on signs, symptoms and biochemical screening. *Eur J Endocrinol*. 2015;173(4):M33-M38.
9. Santos A, Resmini E, Pascual JC, Crespo I, Webb SM. Psychiatric symptoms in patients with Cushing's syndrome: prevalence, diagnosis and management. *Drugs*. 2017;77(8):829-842.
10. Lin TY, Hanna J, Ishak WW. Psychiatric symptoms in Cushing's syndrome: a systematic review. *Innov Clin Neurosci*. 2020;17(1-3):30-35.
11. Michaud K, Forget H, Cohen H. Chronic glucocorticoid hypersecretion in Cushing's syndrome exacerbates cognitive aging. *Brain Cogn*. 2009;71(1):1-8.
12. Broersen LHA, Andela CD, Dekkers OM, Pereira AM, Biermasz NR. Improvement but no normalization of quality of life and cognitive functioning after treatment of Cushing syndrome. *J Clin Endocrinol Metab*. 2019;104(11):5325-5337.
13. Na S, Fernandes MA, Ioachimescu AG, Penna S. Neuropsychological and emotional functioning in patients with Cushing's syndrome. *Behav Neurol*. 2020;2020:4064370.
14. Bourdeau I, Bard C, Forget H, Boulanger Y, Cohen H, Lacroix A. Cognitive function and cerebral assessment in patients who have Cushing's syndrome. *Endocrinol Metab Clin North Am*. 2005;34(2):357-369. ix.
15. Crespo I, Esther GM, Santos A, et al. Impaired decision-making and selective cortical frontal thinning in Cushing's syndrome. *Clin Endocrinol (Oxf)*. 2014;81(6):826-833.
16. Frimodt-Moller KE, Mollegaard Jepsen JR, Feldt-Rasmussen U, Krogh J. Hippocampal volume, cognitive functions, depression, anxiety, and quality of life in patients with Cushing syndrome. *J Clin Endocrinol Metab*. 2019;104(10):4563-4577.
17. Forget H, Lacroix A, Bourdeau I, Cohen H. Long-term cognitive effects of glucocorticoid excess in Cushing's syndrome. *Psychoneuroendocrinology*. 2016;65:26-33.

18. Andela CD, van der Werff SJ, Pannekoek JN, et al. Smaller grey matter volumes in the anterior cingulate cortex and greater cerebellar volumes in patients with long-term remission of Cushing's disease: a case-control study. *Eur J Endocrinol.* 2013;169(6):811-819.
19. van der Werff SJ, Andela CD, Nienke Pannekoek J, et al. Widespread reductions of white matter integrity in patients with long-term remission of Cushing's disease. *Neuroimage Clin.* 2014;4:659-667.
20. Sahut-Barnola I, de Jousineau C, Val P, et al. Cushing's syndrome and fetal features resurgence in adrenal cortex-specific Prkar1a knockout mice. *PLoS Genet.* 2010;6(6):e1000980.
21. Drelon C, Berthon A, Sahut-Barnola I, et al. PKA inhibits WNT signaling in adrenal cortex zonation and prevents malignant tumour development. *Nat Commun.* 2016;7:12751.
22. Dumontet T, Sahut-Barnola I, Septier A, et al. PKA signaling drives reticularis differentiation and sexually dimorphic adrenal cortex renewal. *JCI Insight.* 2018;3(2):e98394.
23. Amaya JM, Suidgeest E, Sahut-Barnola I, et al. Effects of long-term endogenous corticosteroid exposure on brain volume and glial cells in the AdKO mouse. *Front Neurosci.* 2021;15:604103.
24. Paxinos G, Franklin KJB. *The mouse brain in stereotaxic coordinates.* Second Edition. Academic Press; 2001.
25. Gomez-Sanchez CE, Warden M, Gomez-Sanchez MT, Hou X, Gomez-Sanchez EP. Diverse immunostaining patterns of mineralocorticoid receptor monoclonal antibodies. *Steroids.* 2011;76(14):1541-1545.
26. Yao Z, van Velthoven CTJ, Nguyen TN, et al. A taxonomy of transcriptomic cell types across the isocortex and hippocampal formation. *Cell.* 2021;184:3222-3241.e26.
27. Tasic B, Yao Z, Graybeck LT, et al. Shared and distinct transcriptomic cell types across neocortical areas. *Nature.* 2018;563(7729):72-78.
28. Stuart T, Butler A, Hoffman P, et al. Comprehensive integration of single-cell data. *Cell.* 2019;177(7):1888-902 e21.
29. Viho EMG, Buurstede JC, Berkhout JB, Mahfouz A, Meijer OC. Cell type specificity of glucocorticoid signaling in the adult mouse hippocampus. *Journal of Neuroendocrinology.* 2022;34(2):e13072.
30. Makino S, Gold PW, Schulkin J. Corticosterone effects on corticotropin-releasing hormone mRNA in the central nucleus of the amygdala and the parvocellular region of the paraventricular nucleus of the hypothalamus. *Brain Res.* 1994;640(1-2):105-112.
31. Wei F, Song J, Zhang C, et al. Chronic stress impairs the aquaporin-4-mediated glymphatic transport through glucocorticoid signaling. *Psychopharmacology (Berl).* 2019;236(4):1367-1384.
32. Herbert J, Goodyer IM, Grossman AB, et al. Do corticosteroids damage the brain? *J Neuroendocrinol.* 2006;18(6):393-411.
33. Pakdeepak K, Chokchaisiri R, Govitrapong P, Tocharus C, Suksamrarn A, Tocharus J. 5,6,7,4'-Tetramethoxyflavone alleviates neurodegeneration in a dexamethasone-induced neurodegenerative mouse model through promotion of neurogenesis via the Raf/ERK1/2 pathway. *Phytother Res.* 2020;35:2536-2544.
34. Rivers CA, Rogers MF, Stubbs FE, Conway-Campbell BL, Lightman SL, Pooley JR. Glucocorticoid receptor-tethered mineralocorticoid receptors increase glucocorticoid-induced transcriptional responses. *Endocrinology.* 2019;160(5):1044-1056.
35. van Weert L, Buurstede JC, Sips HCM, et al. Identification of mineralocorticoid receptor target genes in the mouse hippocampus. *J Neuroendocrinol.* 2019;31(8):e12735.
36. Mifsud KR, Kennedy CLM, Salatino S, et al. Distinct regulation of hippocampal neuroplasticity and ciliary genes by corticosteroid receptors. *Nat Commun.* 2021;12(1):4737.
37. Ramamoorthy S, Cidlowski JA. Ligand-induced repression of the glucocorticoid receptor gene is mediated by an NCoR1 repression complex formed by long-range chromatin interactions with intragenic glucocorticoid response elements. *Mol Cell Biol.* 2013;33(9):1711-1722.
38. Jenkins SI, Pickard MR, Khong M, et al. Identifying the cellular targets of drug action in the central nervous system following corticosteroid therapy. *ACS Chem Neurosci.* 2014;5(1):51-63.
39. Chetty S, Friedman AR, Taravosh-Lahn K, et al. Stress and glucocorticoids promote oligodendrogenesis in the adult hippocampus. *Mol Psychiatry.* 2014;19(12):1275-1283.
40. Zhou Q, Wang S, Anderson DJ. Identification of a novel family of oligodendrocyte lineage-specific basic helix-loop-helix transcription factors. *Neuron.* 2000;25(2):331-343.
41. Lu QR, Sun T, Zhu Z, et al. Common developmental requirement for Olig function indicates a motor neuron/oligodendrocyte connection. *Cell.* 2002;109(1):75-86.
42. Paes de Faria J, Kessar N, Andrew P, Richardson WD, Li H. New Olig1 null mice confirm a non-essential role for Olig1 in oligodendrocyte development. *BMC Neurosci.* 2014;15:12.
43. Dai J, Bercury KK, Ahrendsen JT, Macklin WB. Olig1 function is required for oligodendrocyte differentiation in the mouse brain. *J Neurosci.* 2015;35(10):4386-4402.
44. Baumann N, Pham-Dinh D. Biology of oligodendrocyte and myelin in the mammalian central nervous system. *Physiol Rev.* 2001;81(2):871-927.
45. Pires P, Santos A, Vives-Gilbert Y, et al. White matter alterations in the brains of patients with active, remitted, and cured Cushing syndrome: a DTI study. *AJNR Am J Neuroradiol.* 2015;36(6):1043-1048.
46. Satoh J, Kino Y, Asahina N, et al. TMEM119 marks a subset of microglia in the human brain. *Neuropathology.* 2016;36(1):39-49.
47. Zalewska K, Ong LK, Johnson SJ, Nilsson M, Walker FR. Oral administration of corticosterone at stress-like levels drives microglial but not vascular disturbances post-stroke. *Neuroscience.* 2017;35230-8:30-38.
48. Jones KA, Zouikr I, Patience M, et al. Chronic stress exacerbates neuronal loss associated with secondary neurodegeneration and suppresses microglial-like cells following focal motor cortex ischemia in the mouse. *Brain Behav Immun.* 2015;48:57-67.
49. Zalewska K, Pietrogrande G, Ong LK, et al. Sustained administration of corticosterone at stress-like levels after stroke suppressed glial reactivity at sites of thalamic secondary neurodegeneration. *Brain Behav Immun.* 2018;69:210-222.
50. Chantong B, Kratschmar DV, Nashev LG, Balazs Z, Odermatt A. Mineralocorticoid and glucocorticoid receptors differentially regulate NF-kappaB activity and pro-inflammatory cytokine production in murine BV-2 microglial cells. *J Neuroinflammation.* 2012;9:260.
51. Li M, Wang Y, Guo R, Bai Y, Yu Z. Glucocorticoids impair microglia ability to induce T cell proliferation and Th1 polarization. *Immunol Lett.* 2007;109(2):129-137.
52. Carter BS, Meng F, Thompson RC. Glucocorticoid treatment of astrocytes results in temporally dynamic transcriptome regulation and astrocyte-enriched mRNA changes in vitro. *Physiol Genomics.* 2012;44(24):1188-1200.
53. Chen KC, Blalock EM, Curran-Rauhut MA, et al. Glucocorticoid-dependent hippocampal transcriptome in male rats: pathway-specific alterations with aging. *Endocrinology.* 2013;154(8):2807-2820.
54. Ye Y, Wang G, Wang H, Wang X. Brain-derived neurotrophic factor (BDNF) infusion restored astrocytic plasticity in the hippocampus of a rat model of depression. *Neurosci Lett.* 2011;503(1):15-19.
55. Lou YX, Li J, Wang ZZ, Xia CY, Chen NH. Glucocorticoid receptor activation induces decrease of hippocampal astrocyte number in rats. *Psychopharmacology (Berl).* 2018;235(9):2529-2540.
56. Simard S, Coppola G, Rudyk CA, Hayley S, McQuaid RJ, Salmaso N. Profiling changes in cortical astroglial cells following chronic stress. *Neuropsychopharmacology.* 2018;43(9):1961-1971.
57. Huet-Bello O, Ruvalcaba-Delgadillo Y, Feria-Velasco A, et al. Environmental noise exposure modifies astrocyte morphology in hippocampus of young male rats. *Noise Health.* 2017;19(90):239-244.
58. Escartin C, Galea E, Lakatos A, et al. Reactive astrocyte nomenclature, definitions, and future directions. *Nat Neurosci.* 2021;24(3):312-325.
59. Xia M, Yang L, Sun G, Qi S, Li B. Mechanism of depression as a risk factor in the development of Alzheimer's disease: the function of AQP4 and the glymphatic system. *Psychopharmacology (Berl).* 2017;234(3):365-379.

60. Li Y, Gu R, Zhu Q, Liu J. Changes of spinal edema and expression of aquaporin 4 in methylprednisolone-treated rats with spinal cord injury. *Ann Clin Lab Sci*. 2018;48(4):453-459.
61. Maatouk L, Yi C, Carrillo-de Sauvage MA, et al. Glucocorticoid receptor in astrocytes regulates midbrain dopamine neurodegeneration through connexin hemichannel activity. *Cell Death Differ*. 2019;26(3):580-596.
62. Dias-Ferreira E, Sousa JC, Melo I, et al. Chronic stress causes frontostriatal reorganization and affects decision-making. *Science*. 2009;325(5940):621-625.
63. Mitra R, Sapolsky RM. Acute corticosterone treatment is sufficient to induce anxiety and amygdaloid dendritic hypertrophy. *Proc Natl Acad Sci USA*. 2008;105(14):5573-5578.
64. Eun SY, Hong YH, Kim EH, et al. Glutamate receptor-mediated regulation of c-fos expression in cultured microglia. *Biochem Biophys Res Commun*. 2004;325(1):320-327.
65. Shimoyama S, Furukawa T, Ogata Y, et al. Lipopolysaccharide induces mouse translocator protein (18 kDa) expression via the AP-1 complex in the microglial cell line, BV-2. *PLoS One*. 2019;14(9):e0222861.
66. Herman JP, Nawreen N, Smail MA, Cotella EM. Brain mechanisms of HPA axis regulation: neurocircuitry and feedback in context Richard Kvetnansky lecture. *Stress*. 2020;23(6):617-632.
67. Boscaro M, Barzon L, Fallo F, Sonino N. Cushing's syndrome. *Lancet*. 2001;357(9258):783-791.
68. Yasuda K, Maki T, Kinoshita H, et al. Sex-specific differences in transcriptomic profiles and cellular characteristics of oligodendrocyte precursor cells. *Stem Cell Res*. 2020;46101866:101866.
69. Guneykaya D, Ivanov A, Hernandez DP, et al. Transcriptional and translational differences of microglia from male and female brains. *Cell Rep*. 2018;24(10):2773-83 e6.
70. Gall CM, Le AA, Lynch G. Sex differences in synaptic plasticity underlying learning. *J Neurosci Res*. 2021;1-19.
71. Taqi MO, Saeed-Zidane M, Gebremedhn S, et al. Sexual dimorphic expression and release of transcription factors in bovine embryos exposed to oxidative stress. *Mol Reprod Dev*. 2019;86(12):2005-2019.

SUPPORTING INFORMATION

Additional supporting information may be found in the online version of the article at the publisher's website.

How to cite this article: Amaya JM, Viho EMG, Sips HCM, et al. Gene expression changes in the brain of a Cushing's syndrome mouse model. *J Neuroendocrinol*. 2022;34(4):e13124. doi:10.1111/jne.13125